

# Highly excited states of *gerade* symmetry in molecular nitrogen

Arno de Lange

*Laser Centre, Department of Physics and Astronomy, Vrije Universiteit, Amsterdam, The Netherlands*

Rüdiger Lang

*Laser Centre, Department of Physics and Astronomy, Vrije Universiteit, Amsterdam, The Netherlands  
and FOM Institute for Atomic and Molecular Physics, Amsterdam, The Netherlands*

Wim van der Zande

*FOM Institute for Atomic and Molecular Physics, Amsterdam, The Netherlands*

Wim Ubachs

*Laser Centre, Department of Physics and Astronomy, Vrije Universiteit, Amsterdam, The Netherlands*

(Received 24 September 2001; accepted 18 February 2002)

Highly excited states of *gerade* symmetry in molecular nitrogen have been investigated in a resonance-enhanced XUV+Vis (extreme ultraviolet+visible) transition scheme. Nineteen bands have been observed, of which only four involve known states [ $k^1\Pi_g$  ( $v=1$ ),  $x^1\Sigma_g^-$  ( $v=2$ ), and  $y^1\Pi_g$  ( $v=1,2$ )], albeit in new systems. Three of the newly observed states have been assigned as  $y^1\Pi_g$  ( $v=3$ ) and  $k^1\Pi_g$  ( $v=2,3$ ). Level energies are determined with an accuracy of  $\approx 0.20$   $\text{cm}^{-1}$ . © 2002 American Institute of Physics. [DOI: 10.1063/1.1468220]

## I. INTRODUCTION

At excitation energies between  $\approx 100\,000$   $\text{cm}^{-1}$  and the first ionization limit ( $125\,666$   $\text{cm}^{-1}$ ), molecular nitrogen exhibits a complex and congested spectrum, which was observed in absorption<sup>1</sup> and partly in emission.<sup>2,3</sup> This spectrum was extensively studied by Lefebvre-Brion,<sup>4</sup> Dressler,<sup>5</sup> and Carroll, Collins, and Yoshino<sup>6,7</sup> and it is established now that it can be explained in terms of two valence states,  $b'^1\Sigma_u^+$  and  $b^1\Pi_u$ , two Rydberg series  $c_n'^1\Sigma_u^+$  and  $c_n^1\Pi_u$  which both converge to the first ionization limit and the Rydberg series  $o_n^1\Pi_u$  converging to the  $A^2\Pi_u$  excited state of the  $\text{N}_2^+$  ion.<sup>8</sup>

A similar structure is to be expected for the *gerade* manifold, but investigations in the past have been sparse due to the fact that transitions from the electronic ground state to these *gerade* states are dipole forbidden. Emission experiments in discharges have been performed in the past, from which some information about the *gerade* states has been obtained. More recently, laser excitation experiments involving *gerade* excited states have been performed as well. Besides the ground state, up to now only six singlet *gerade* states have been observed and identified in molecular nitrogen:  $a^1\Pi_g$ ,  $a''^1\Sigma_g^+$ ,  $x^1\Sigma_g^-$ ,  $y^1\Pi_g$ ,  $k^1\Pi_g$ , and  $z^1\Delta_g$ . The MO (molecular orbit) configurations are tabulated in Table I. The  $a^1\Pi_g$  state is a valence state whereas the other five states are Rydberg states.

The first excited singlet *gerade* state observed, was the  $a^1\Pi_g$  state. This state was first detected in emission in the  $a^1\Pi_g-X^1\Sigma_g^+$  system by Lyman in 1911.<sup>9</sup> More bands were added to this system by Birge and Hopfield<sup>10</sup> who also analyzed the vibrational structure. The system has become known as the Lyman–Birge–Hopfield system. In 1965 Vanderslice *et al.*<sup>11</sup> obtained the absorption spectrum at high accuracy and Ref. 11 was the most important reference for several decades. Some of the bands, observed in absorption,

were analyzed at even higher accuracy by Miller.<sup>12</sup> In recent years this system was reinvestigated in a resonance enhanced multi-photon ionization (REMPI) scheme<sup>13</sup> and in emission.<sup>14</sup> The  $a$  state was also observed in some other systems by Gaydon and Herman<sup>15–19</sup> (Gaydon–Herman singlet systems;  $b^1\Pi_u-a^1\Pi_g$ ,  $b'^1\Sigma_u^+-a^1\Pi_g$ ,  $c_3^1\Pi_u-a^1\Pi_g$ ,  $c_4^1\Pi_u-a^1\Pi_g$ ,  $c_4'^1\Sigma_u^+-a^1\Pi_g$ , and  $o^1\Pi_u-a^1\Pi_g$ ) and McFarlane<sup>20–23</sup> (McFarlane infrared system;  $a^1\Pi_g-a'^1\Sigma_u^-$  and  $w^1\Delta_u-a^1\Pi_g$ ).

The existence of the  $a''^1\Sigma_g^+$  state was first predicted by Mulliken<sup>24</sup> in 1957. Lefebvre-Brion and Moser<sup>25</sup> estimated that this state can be observed in absorption by quadrupole transitions or pressure induced dipole transitions from the ground state. Dressler and Lutz observed this transition in 1967.<sup>26</sup> In an investigation of Rydberg states, Ledbetter<sup>27</sup> obtained molecular constants for several vibrational levels in the  $a''$  state, which were the most accurate for many years. Suzuki and Kakimoto<sup>28</sup> improved the rotational constants for  $v=0$  in 1981, but more accurate data on higher vibrational levels were obtained from new experiments only in the last decade<sup>29,30</sup>

Duncan observed in 1925<sup>31</sup> for the first time the  $x^1\Sigma_g^-$  state in the fifth positive system ( $x^1\Sigma_g^- - a'^1\Sigma_u^-$ ), but did not make any assignments in terms of electronic character. Neither did Appleyard, who added several more bands to this system.<sup>32</sup> Van der Ziel<sup>33</sup> performed a rotational analysis of the bands, and assigned the correct symmetry to the state;  $^1\Sigma_g^-$ . Gaydon<sup>15</sup> pointed out that the symmetry of the  $x$  state also could be  $^1\Sigma_u^+$ , however, theoretical considerations<sup>24</sup> favored the assignment of  $^1\Sigma_g^-$ . The most accurate measurements were performed by Lofthus.<sup>34</sup>

Though Duncan<sup>31</sup> observed the  $y^1\Pi_g$  state for the first time in 1925, it was Kaplan<sup>35–37</sup> who recognized the regularities in 1934 and the two observed systems were later referred as Kaplan first system ( $y^1\Pi_g - a'^1\Sigma_u^-$ ) and Kaplan

TABLE I. The molecular orbit (MO) configurations of the known singlet *gerade* states.

$X^1\Sigma_g^+$	$(1\sigma_g)^2(1\sigma_u)^2(2\sigma_g)^2(2\sigma_u)^2(1\pi_u)^4(3\sigma_g)^2$
$a^1\Pi_g$	$(1\sigma_g)^2(1\sigma_u)^2(2\sigma_g)^2(2\sigma_u)^2(1\pi_u)^4(3\sigma_g)^1(1\pi_g)^1$
$a''^1\Sigma_g^+$	$(1\sigma_g)^2(1\sigma_u)^2(2\sigma_g)^2(2\sigma_u)^2(1\pi_u)^4(3\sigma_g)^1 Ry\ 3s\sigma_g$
$x^1\Sigma_g^-$	$(1\sigma_g)^2(1\sigma_u)^2(2\sigma_g)^2(2\sigma_u)^2(1\pi_u)^3(3\sigma_g)^2 Ry\ 3p\pi_u$
$y^1\Pi_g$	$(1\sigma_g)^2(1\sigma_u)^2(2\sigma_g)^2(2\sigma_u)^2(1\pi_u)^3(3\sigma_g)^2 Ry\ 4p\sigma_u$
$k^1\Pi_g$	$(1\sigma_g)^2(1\sigma_u)^2(2\sigma_g)^2(2\sigma_u)^2(1\pi_u)^4(3\sigma_g)^1 Ry\ 4d\pi_g$
$z^1\Delta_g$	$(1\sigma_g)^2(1\sigma_u)^2(2\sigma_g)^2(2\sigma_u)^2(1\pi_u)^3(3\sigma_g)^2 Ry\ 3p\pi_u$

second system ( $y^1\Pi_g-w^1\Delta_u$ ). Gaydon performed a rotational analysis of Kaplan's first system, and assigned either the  $^1\Pi_g$  or  $^1\Pi_u$  label to the  $y$  state. Lofthus and Mulliken<sup>38</sup> remeasured both systems under high accuracy and settled the final assignment of the  $y$  state to  $^1\Pi_g$ . Strong perturbations in the rotational progressions for both vibrational levels  $v=0,1$  were observed. Beside this, some of the (*e*) components of the  $v=0$  state and all of the (*e*) components of the  $v=1$  state were missing in the spectra. Carroll and Subbaram<sup>39</sup> showed that the perturbations arise from an interaction with the  $k^1\Pi_g$  state. Furthermore, an indirect pre-

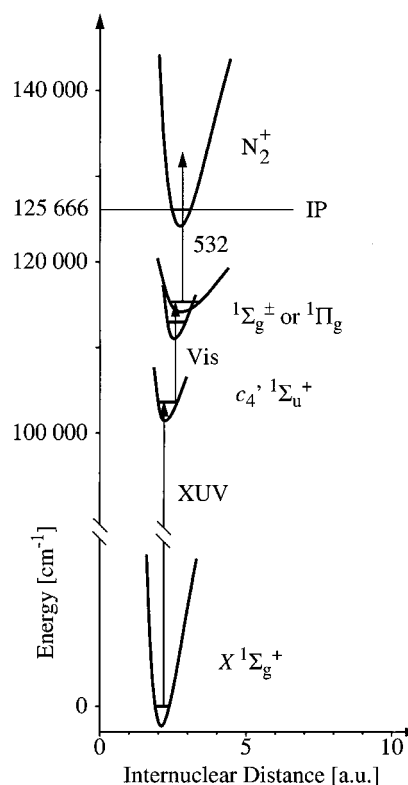


FIG. 2. A transition scheme of the experiment. An XUV photon of  $\approx 96$  nm is used to populate a specific rotational level of the  $c_4'^1\Sigma_u^+$  ( $v=0$ ) state. A second laser scans the wavelength region of  $\lambda=620$ – $970$  nm to probe singlet *gerade* states between  $114\,500$ – $120\,200$   $\text{cm}^{-1}$ .  $N_2$  molecules in these highly excited states, are finally ionized by the second harmonic of a Nd:YAG laser (532 nm).

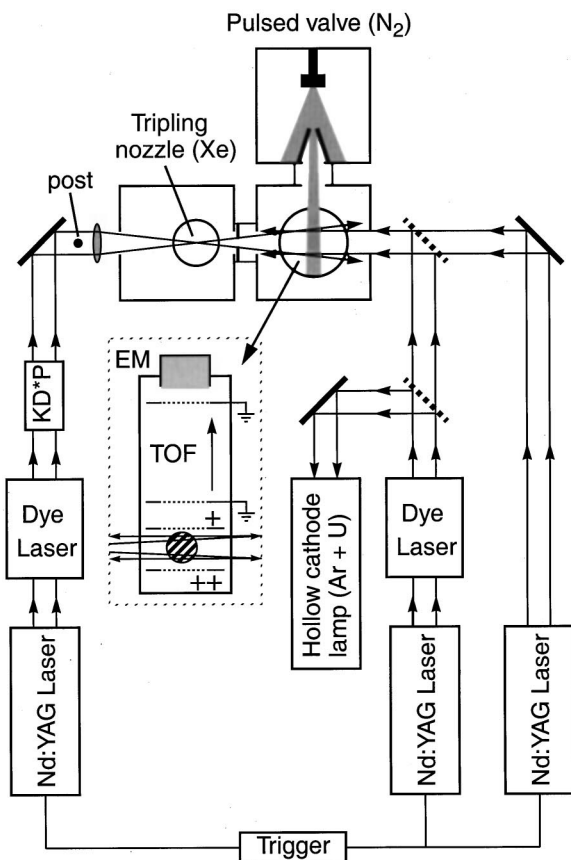


FIG. 1. Scheme of the experimental setup. XUV radiation is generated by frequency doubling, and subsequent tripling of the output of a pulsed dye laser. This radiation is used to drive the transition from the ground state to a specific rotational level of the intermediate  $c_4'^1\Sigma_u^+$  ( $v=0$ ) state. The radiation of a second pulsed dye laser is exploited as probe laser for the highly excited singlet *gerade* states. Finally, a third laser, the second harmonic of Nd:YAG (532 nm), is used to ionize the  $N_2$  molecules in these highly excited states. These ions are accelerated, mass-selected, and detected in a time of flight setup (see inset). The wavelength of the second laser is calibrated online against a U-Ar standard.

dissociation mechanism was proposed to explain the missing (*e*) components. All these experiments were emission experiments. Recently, the (*e*) components were observed in a double resonance experiment by de Lange and Ubachs.<sup>40</sup> The predissociation mechanism proposed by Carroll and Subbaram was supported by their analysis.

The  $k^1\Pi_g$  state was first observed by Carroll and Subbaram<sup>39</sup> and their names were given to two systems:  $k^1\Pi_g-a'^1\Sigma_u^-$  (Carroll–Subbaram first system) and  $k^1\Pi_g-w^1\Delta_u$  (Carroll–Subbaram second system). Similar perturbations as in the  $y$  state were observed, which can be explained by a mutual interaction between those states.<sup>39</sup> Also in the case of the  $k$  state, the (*e*) components of  $v=1$  were missing in the emission spectra of Carroll and Subbaram, but were observed in the laser excitation spectra by de Lange and Ubachs.<sup>40</sup>

Finally, the sixth identified singlet *gerade* state is the  $z^1\Delta_g$  state. This state was observed by Lofthus in 1957<sup>41</sup> in emission. Although this is the only reported observation up to our knowledge, the state is also found in the *ab initio* calculations of Michels.<sup>42</sup>

In this paper we report on a two-photon laser excitation study, with subsequent photo-ionization by a third laser pulse. As a result 19 vibronic systems of *gerade* symmetry were identified of which 15 were hitherto unobserved. Since no *ab initio* potential energy curves of spectroscopic accuracy are available and because, similar to the case of *unger-*

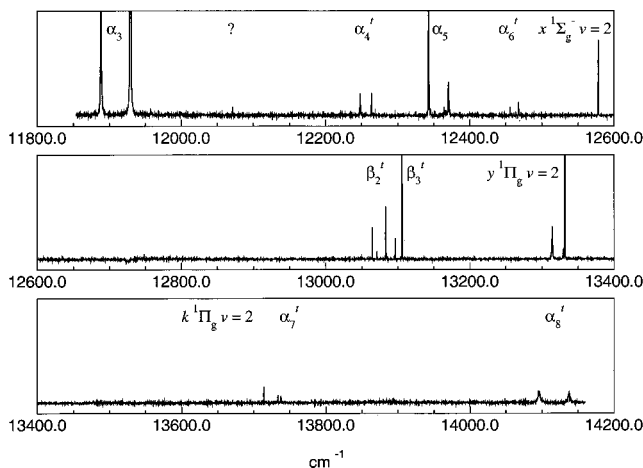


FIG. 3. An overview spectrum of part of the investigated wavelength region. The XUV laser is tuned such that the  $c_4' \ ^1\Sigma_u^+$  ( $v=0, J=5$ ) level at  $104\,380.42\text{ cm}^{-1}$  is populated. The second laser is scanned from  $11\,800\text{--}14\,200\text{ cm}^{-1}$ . One feature in the spectrum is not assigned and this is indicated with (?).

*ade* symmetry states in this energy region, strong perturbations are expected, no definite vibronic assignment of the features can be made. However, as a helpful feature of double resonance spectroscopy the assignment in terms of rotational quantum numbers can be given unambiguously in virtually all cases. Moreover, based on estimates of vibrational spacings newly observed *gerade* vibronic systems were assigned, albeit tentatively, as  $y \ ^1\Pi_g$  ( $v=3$ ) and  $k \ ^1\Pi_g$  ( $v=2,3$ ).

## II. EXPERIMENT

The general features of the experimental setup are the same as the one used in a previous investigation focusing on the  $k \ ^1\Pi_g$  and  $y \ ^1\Pi_g$  states.<sup>40</sup> A schematic overview of the setup is depicted in Fig. 1. Tunable XUV laser light ( $\lambda \approx 96\text{ nm}$ ) is generated by frequency doubling the output of a PDL (pulsed dye laser) into ultraviolet in a KDP crystal, and subsequently frequency tripling the output in a xenon gas jet. This XUV radiation is used to populate a single rotational quantum state in the  $c_4' \ ^1\Sigma_u^+$  ( $v=0$ ) state, which was used as an intermediate. The second beam, the probe beam, was spatially overlapped with the XUV beam and in view of the short life time of the  $c_4'$  state [ $\approx 1\text{ ns}$  (Ref. 43)] also temporally overlapped. The wavelength of this second beam covered the range of  $620\text{--}970\text{ nm}$  generated by a second PDL, enabling us to investigate the energy region of  $114\,500\text{--}120\,200\text{ cm}^{-1}$  above the ground state. The transition scheme used in this experiment is shown in Fig. 2. The wave function of the intermediate state is located at small internuclear distances, restricting the possible states that can be investigated. Only states with sufficient wave function density at these small internuclear distances can be probed.

Whereas a Te<sub>2</sub> absorption spectrum was used for calibration purposes in the experiment of Ref. 40, in the current investigation an argon-filled hollow uranium cathode lamp was used. The advantage of this calibration method is the large wavelength region that can be covered, but unfortu-

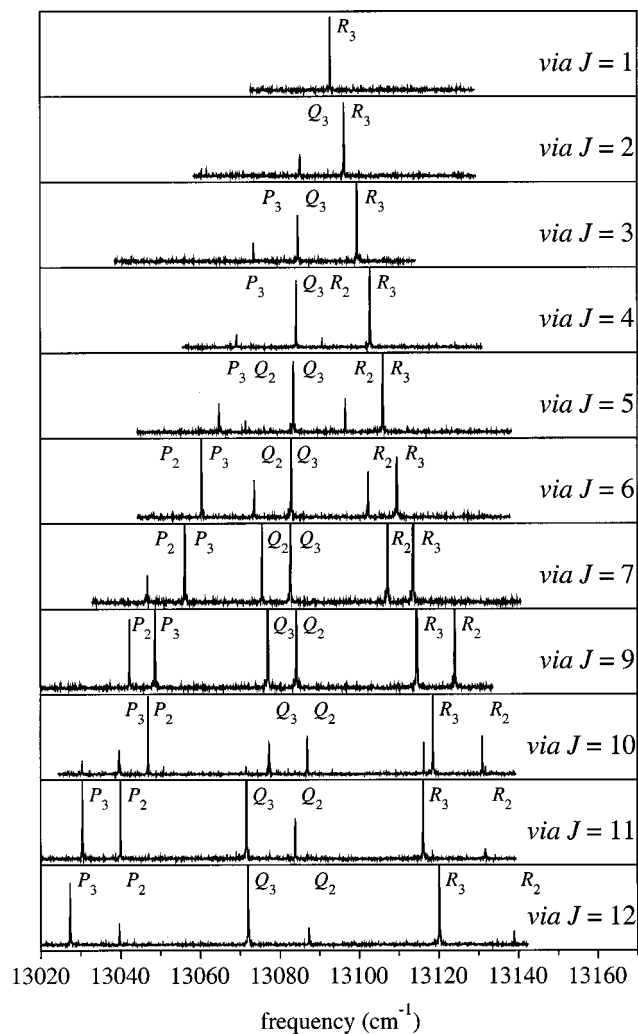


FIG. 4. Observed spectra, via different rotational levels of the intermediate state  $c_4' \ ^1\Sigma_u^+$  ( $v=0$ ). The transitions  $X \ ^1\Sigma_g^+$  ( $v=0$ )  $- c_4' \ ^1\Sigma_u^+$  ( $v=0$ )  $P(11)$  and  $P(12)$  are partially overlapped and both transitions will occur when the XUV laser is set on either one of the resonances. This results in additional lines which are indicated with an asterisk.

nately the resulting accuracy is somewhat less ( $\approx 0.20\text{ cm}^{-1}$ ) than in the case of Te<sub>2</sub> absorption ( $\approx 0.05\text{ cm}^{-1}$ ). A third laser pulse (532 nm) further excites the N<sub>2</sub> molecules into the ionization continuum, therewith producing N<sub>2</sub><sup>+</sup> ions that can be sensitively detected. The third laser pulse was both spatially and temporally overlapped.

Double resonance spectra were obtained by setting the tunable XUV laser on one of the rotational lines in the  $c_4' \ ^1\Sigma_u^+ - X \ ^1\Sigma_g^+$  (0,0) band and keeping it fixed, while scanning the second laser in the visible wavelength domain. Signal is obtained by monitoring the N<sub>2</sub><sup>+</sup> ion yield as a function of wavelength, resulting in a typical double resonance spectra as shown in Fig. 3. In this figure six up to now unobserved  $^1\Sigma_g^+$  states ( $\alpha_3\text{--}\alpha_8$ ) are depicted along with three new  $^1\Pi_g$  states [ $\beta_2, \beta_3$  and  $k$  ( $v=2$ )]. The vibrational levels  $v=2$  of the  $y$  state and  $v=2$  of the  $x$  state were already known. One feature in Fig. 3 is not identified. The intensity of the laser radiation is not diminished, resulting in possibly broadened lines. For instance band  $\alpha_8'$  seems to be broadened, but this does not necessarily imply a short lived level.

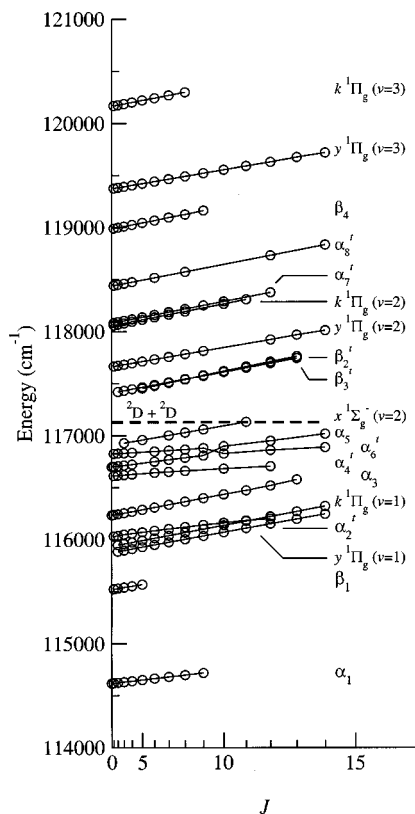


FIG. 5. An overview of all observed levels, plotted here with rotational quantum number unambiguously assigned. Four vibronic states have been observed before  $x^1\Sigma_g^-(v=2)$ ,  $y^1\Pi_g(v=1,2)$ , and  $k^1\Pi_g(v=1)$ . Three states are tentatively assigned to higher vibrational levels of known electronic states:  $y^1\Pi_g(v=3)$  and  $k^1\Pi_g(v=2,3)$ .

Figure 4 displays spectra to the levels named  $\beta_2$  and  $\beta_3$  for various intermediate  $J$  levels. Although there is some irregularity in the intensity patterns, two series of  $P$ ,  $Q$ , and  $R$  transitions are discernable. All recorded spectra reflect the well-known perturbation in the  $c_4^1\Sigma_u^+(v=0)$  state by the  $b^1\Sigma_u^+(v=1)$  state with an avoided crossing near  $J=10$ . This is observable in Fig. 4 through the shifts of some lines and by the appearance of additional lines, due to the fact that

TABLE II. Level energies positively assigned as vibrational levels of  $^1\Sigma_g^+$  states.

$J$	$\alpha_1$	$\alpha_3$	$\alpha_5$
0	114 617.40	116 234.50	116 700.68
1	114 619.71	116 237.52	116 702.69
2	114 624.32	116 244.55	116 707.52
3	114 631.32	116 255.13	116 714.32
4	114 640.38	116 269.51	116 723.63
5	114 652.11	116 288.20	
6	114 665.36	116 310.00	116 751.20
7	114 681.65	116 336.51	116 768.77
8	114 699.41	116 366.14	116 788.24
9	114 719.40	116 399.70	116 808.94
10		116 436.35	116 899.28
11		116 474.28	
12		116 521.05	116 951.04
13		116 579.30	
14			117 017.95

TABLE III. Level energies of  $x^1\Sigma_g^-(v=2)$ .

$J$	$x^1\Sigma_g^-(v=2)$
3	116 928.26
5	116 958.69
7	117 002.88
8	117 030.12
9	117 060.33
11	117 131.60

the resonances in the first excitation step cannot be resolved. We note however, that the perturbation in  $c_4^1(v=0)$  is fully understood and modeled; it has no effect on the assignment and accuracy in the double resonance spectra.

Although all three lasers are both temporally and spatially overlapped, unambiguous assignments of the quantum states excited, can be made. All signal is dependent on the first XUV-resonant excitation step, while XUV+green does not yield ion signal; the observed resonances in the  $N_2$  spectrum rely on the tuning of the second laser. In some incidental cases signal was obtained, however, that was independent of the 532 nm pulse and which was attributed to XUV+Vis+Vis excitation. In these cases a resonance at the XUV+Vis energy level would not be required, and the signal could be produced by autoionizing levels at the XUV+2 Vis energy level. All spectra were recorded by monitoring molecular ion signal at mass 28. Atomic fragments are produced in cases when a predissociating state is probed; these fragments are not detected since they are electrically neutral.

### III. RESULTS AND DISCUSSION

Nineteen rotational progressions have been discerned, of which four were already known [ $x^1\Sigma_g^-(v=2)$ ,  $y^1\Pi_g(v=1,2)$ , and  $k^1\Pi_g(v=1)$ ]. The level energies were determined by adding the calibrated transition energies to the level energies of the intermediate  $c_4^1\Sigma_u^+$  state. The latter are known within  $\approx 0.03$   $\text{cm}^{-1}$ .<sup>44</sup> The observed energy levels are shown in Fig. 5. The energies of all observed levels are listed in Tables II–VIII, except for  $k^1\Pi_g(v=1)$  and  $y^1\Pi_g(v=1)$ , which can be found in Ref. 40, with an accuracy of  $\approx 0.04$   $\text{cm}^{-1}$ . The energies are listed rather than the transition frequencies to bypass the perturbations in the intermediate state.

TABLE IV. Level energies positively assigned as vibrational levels of  $^1\Pi_g$  states.

$J$	$\beta_1$		$\beta_4$	
	(e)	(f)	(e)	(f)
1	115 524.87	115 524.30	118 989.78	118 990.47
2	115 531.02	115 531.02	118 997.72	118 997.56
3	115 540.85		119 008.98	119 009.63
4		115 553.82	119 024.32	119 025.13
5	115 569.53		119 043.31	119 045.52
6			119 066.12	
7				119 095.47
8			119 124.36	
9				119 162.01

TABLE V. Level energies of the  $y^1\Pi_g$  ( $v=2,3$ ) states.  $v=2$  was already observed before,  $v=3$  is observed for the first time.

$J$	$y^1\Pi_g$ ( $v=2$ )		$y^1\Pi_g$ ( $v=3$ )	
	( $e$ )	( $f$ )	( $e$ )	( $f$ )
1	117 664.75	117 664.80	119 375.84	119 375.90
2	117 671.45	117 671.53	119 382.51	119 382.33
3	117 681.54	117 681.78	119 392.38	119 392.56
4	117 694.47		119 405.61	119 405.99
5	117 711.57	117 712.38	119 422.30	119 422.89
6	117 731.58	117 732.48	119 442.03	
7	117 754.81	117 756.19		119 465.89
8	117 781.01	117 783.37	119 491.43	
9	117 811.67	117 813.77	119 521.04	119 522.75
10			119 554.08	119 555.92
11			119 590.63	119 592.67
12	117 922.64		119 630.14	
13		117 969.42		119 676.31
14	118 012.11		119 719.92	

The assignment of all observed spectral features in terms of electronic symmetries and rovibrational quantum numbers is a difficult task. *Ab initio* calculations<sup>42</sup> have been performed resulting in Born–Oppenheimer (BO) potential curves, but not to the level of spectroscopic accuracy required for unambiguous assignments of levels. However, the nature of the double-resonance excitation scheme gives some help in the assignments. The rotational quantum numbers of the newly observed levels are known without ambiguity. This holds foremost for those levels observed in  $P$  and  $R$  transitions, but also the ones observed in a single transition (e.g.,  $Q$  branch lines) follow clearly rotational progressions.

In view of the excitation scheme, the features studied here have singlet character and *gerade* symmetry. Furthermore, the states that can be probed from the  $c_4^1\Sigma_u^+$  are constrained by dipole selection rules. Only rovibrational levels of  $^1\Sigma_g^+$  and  $^1\Pi_g$  states can be populated.  $P$  and  $R$  transitions probe either  $\Sigma^+$  or  $\Pi(e)$  states, whereas  $Q$  transitions probe  $\Pi(f)$  states.  $P$  and  $R$  transitions both populate identical levels and therefore combination differences can be used to yield higher accuracies than in the case of  $Q$  transitions ( $\approx 0.15\text{ cm}^{-1}$  and  $\approx 0.20\text{ cm}^{-1}$ , respectively). On the basis of observed transitions a tentative symmetry assignment has

TABLE VI. Level energies of the  $k^1\Pi_g$  ( $v=2,3$ ) states. Both vibrational levels were hitherto unobserved.

$J$	$k^1\Pi_g$ ( $v=2$ )		$k^1\Pi_g$ ( $v=3$ )	
	( $e$ )	( $f$ )	( $e$ )	( $f$ )
1	118 060.27			120 167.79
2		118 068.00	120 175.11	
3	118 079.38	118 079.38		120 186.58
4	118 094.42	118 094.95	120 201.66	
5	118 113.42	118 113.98		120 221.13
6	118 136.16	118 136.84	120 242.31	
7	118 162.30	118 163.54		120 269.34
8	118 192.39	118 193.58	120 298.24	
9				
10	118 265.07			
11		118 309.30		

TABLE VII. Level energies of states tentatively assigned as  $^1\Pi_g$ . It is, however, possible that band  $\beta_2^t$  probes a  $^1\Delta_g$  state, as is explained in the text. Of neither state a  $J=1$  rotational level has been observed, leaving the assignment tentative.

$J$	$\beta_2^t$		$\beta_3^t$	
	( $e$ )	( $f$ )	( $e$ )	( $f$ )
2			117 419.33	117 419.36
3			117 430.48	117 430.42
4			117 445.32	117 445.49
5	117 451.94	117 451.95	117 463.98	117 463.96
6	117 477.11	117 477.10	117 486.51	117 486.43
7	117 505.81	117 505.86	117 513.04	117 513.05
8	117 537.53		117 543.91	
9	117 579.29	117 579.36	117 572.00	117 572.16
10	117 619.14	117 619.28	117 609.61	117 609.70
11	117 663.18	117 662.86	117 650.82	117 650.60
12	117 710.69	117 710.47	117 695.12	117 695.13
13	117 762.06		117 743.30	

been given. If the  $P(1)$  transition is observed, the probed state has to be a  $^1\Sigma_g^+$  state; only  $\Sigma$  states support a  $J=0$  rotational level, and only  $\Sigma^+$  can be probed via a  $P$  transition. And, if  $P$ ,  $Q$ , and  $R$  transitions are all observed, the probed state must be  $^1\Pi_g$ . It might of course be that, in the case of a  $\Pi$  state, either the  $P/R$  or  $Q$  branch is missing, due to the predissociation of either the ( $e$ ) or ( $f$ ) component which would lead to ambiguities in the assignment. Furthermore, it is possible that the lowest rotational level is not discerned, which also may lead to equivocalities. Based on this scheme, three  $^1\Sigma_g^+$  states ( $\alpha_1, \alpha_3$ , and  $\alpha_5$ ) have been unambiguously assigned, as well as six  $^1\Pi_g$  states [ $\beta_1, \beta_4, y$  ( $v=1-3$ ), and  $k$  ( $v=1-3$ )]. In five cases ( $\alpha_2^t, \alpha_4^t, \alpha_6^t, \alpha_7^t$ , and  $\alpha_8^t$ ) only a  $P$  and  $R$  branch is observed, but  $J=0$  has not been measured, leaving the final assignment still unclear. In two cases ( $\beta_2^t$  and  $\beta_3^t$ ) all three branches are observed, but not  $J=1$ . Finally a  $Q$  branch is observed which coincides with the levels of the  $x^1\Sigma_g^-$  ( $v=2$ ) state. This is peculiar as a  $^1\Sigma_g^- - ^1\Sigma_u^+$  transition is dipole forbidden. Probably some transition strength is gained from an interac-

TABLE VIII. Level energies of states tentatively assigned as  $^1\Sigma_g^+$ . Only  $P$  and  $R$  branches are observed in the following bands. However, no  $J=0$  level has been observed, leaving the assignment tentative. It may be that the probed states are of  $^1\Pi_g$  ( $e$ ) signature.

$J$	$\alpha_2^t$	$\alpha_4^t$	$\alpha_6^t$	$\alpha_7^t$	$\alpha_8^t$
1	116 031.15	116 613.71	116 827.26	118 084.35	118 441.99
2	116 036.58	116 617.29	116 829.37	118 091.74	118 449.77
3	116 049.29	116 622.25	116 832.31	118 103.28	118 460.94
4	116 058.92	116 628.40	116 836.56	118 118.36	118 475.98
5	116 071.35			118 137.46	
6	116 085.94	116 643.95	116 848.57	118 160.20	118 517.48
7	116 102.53	116 652.91	116 856.79	118 186.70	
8	116 121.29	116 662.42	116 867.29	118 217.11	118 574.26
9	116 141.24		116 881.02	118 251.18	
10	116 162.11	116 683.24	116 828.71	118 289.21	
11	116 184.98				
12	116 203.19	116 706.45	116 862.24	118 376.22	118 731.97
13					
14			116 889.54		118 834.58

TABLE IX. Molecular parameters of the unassigned states along with the parameters of the ground state and the first excited state of  $N_2^+$ . All values are in  $\text{cm}^{-1}$ .

System	$\nu$	$B$	$D$ ( $10^{-3}$ )	$Q$	$\chi^2$
$\alpha_1$	114 617.30(12)	1.176(8)	0.47(9)		0.13
$\beta_1$	115 521.14(21)	1.65(4)	1.3(1.1)		1.63
$\alpha'_2$	116 033.60(16)	0.750(3)	1.13(5)	0.545(3)	2.28
$\alpha_3$	116 234.21(6)	1.775(2)	-0.55(14)		48.07
$\alpha'_7$	118 080.50(10)	1.896(2)			0.10
$\alpha'_8$	118 438.29(10)	1.886(1)			0.84
$\beta_4$	118 985.88(7)	1.956(3)		-0.037(3)	0.46
States of the $N_2^+$ ion					
$X^2\Sigma_g^+$					
$\nu=0$	0.00	1.922	0.0057		
$\nu=1$	2174.75	1.903	0.0058		
$\nu=2$	4316.98	1.884	0.0058		
$\nu=3$	6426.46	1.865	0.0060		
$A^2\Pi_u$					
$\nu=0$	9016.00	1.735	0.0056		
$\nu=1$	10 889.45	1.716	0.0057		
$\nu=2$	12 732.83	1.697	0.0056		
$\nu=3$	14 546.17	1.678			

tion with a  $^1\Pi_g$  state. The levels which could not be identified as vibrational levels of known states, are labeled as  $\alpha_i$  in the case of a  $\Sigma$  state with the index  $i$  as an arbitrary label, numbering the states from low to high energies. The  $\Pi$  states are called  $\beta_i$ . A  $t$  superscript is added if the assignment is tentative.

The rotational level energies of the unperturbed  $\Sigma$  states are fitted to the following formula:

$$E = \nu + BJ(J+1) - DJ^2(J+1)^2. \quad (1)$$

In the case of  $\Pi$  states  $\Lambda$  doubling will occur and the rotational level energies are fitted to the set of equations

$$E_e = \nu + (B+Q)J(J+1) - DJ^2(J+1)^2, \\ E_f = \nu + BJ(J+1) - DJ^2(J+1)^2. \quad (2)$$

The results from least-squares fits of the data to these equations are listed in Tables IX–XI. The centrifugal distortion

TABLE X. Molecular parameters of the assigned vibrational levels. All values are in  $\text{cm}^{-1}$ .

$\nu$	$\nu$	$B$	$D$ ( $10^{-3}$ )	$Q$	$\chi^2$
$x^1\Sigma_g^-$					
2	116 907.93(16)	1.695(2)			0.22
$y^1\Pi_g$					
2	117 661.39(6)	1.693(1)		-0.023(1)	1.13
3	119 372.46(6)	1.669(1)		-0.016(1)	0.80
$k^1\Pi_g$					
2	118 056.30(15)	1.934(11)	0.34(16)	-0.020(4)	0.40
3	120 163.86(9)	1.906(11)	0.34(16)	-0.017(5)	2.16

TABLE XI. The molecular parameters of the interacting states  $\beta_2^t$  and  $\beta_3^t$ . All values are in  $\text{cm}^{-1}$ .

System	$\nu$	$B$	$D$ ( $10^{-3}$ )	$H_{\beta_2^t\beta_3^t}$
Heterogeneous interaction assumed				
$\beta_2^t$	117 389.05(24)	2.129(6)	0.49(3)	0.363(8)
$\beta_3^t$	117 408.23(8)	1.849(1)		0.363(8)
$\chi^2=0.36$				
Homogeneous interaction assumed				
$\beta_2^t$	117 389.59(26)	2.130(6)	0.48(3)	3.13(7)
$\beta_3^t$	117 407.70(9)	1.847(1)		3.13(7)
$\chi^2=0.36$				

parameter was set to  $D=0$  in the case that the adding of this parameter did not result in a lowering of the  $\chi^2$ .

From the intermediate  $c_4^1\Sigma_u^+$  state, both valence states and Rydberg states can be probed. In the former case, an electron is excited from a bonding orbital to an antibonding orbital, resulting in an increase of the internuclear distance, whereas in the latter case, an electron is excited to an orbital in which it experiences significantly less influence from the nuclei than the other electrons, and the nuclear distance will resemble the distance of an ionic state. As the molecular constants depend on the internuclear distance, these can be used to interpret the character of the observed states. In a Rydberg series, the Rydberg electron occupies orbitals with increasing principal quantum numbers, and finally the series converges to an ionic state. It is therefore to be expected that the molecular constants of such a series also converge to the constants of the ionic state. In Table IX the constants of the ground state and the first excited state of the molecular ion<sup>45–48</sup> are listed.

Based on the rotational  $B$  parameter, a first crude assignment can be made on the character of the excited state. It seems that states  $\beta_3^t$ ,  $\alpha_7^t$ ,  $\alpha_8^t$ , and  $\beta_4$  belong to Rydberg series converging to the electronic ground state of the  $N_2^+$  ion. Bands  $\alpha_1^t$ ,  $\beta_1$ ,  $\alpha_2^t$ ,  $\alpha_4$ ,  $\alpha_5$ , and  $\alpha_6$  have relative small rotational  $B$  parameters, indicating that the internuclear distance must be relatively large corresponding to valence states. Band  $\alpha_3$ , with  $B=1.775 \text{ cm}^{-1}$ , is just between the values of the rotational constant of the ground state and the first excited state of  $N_2^+$ . However, it seems that the rotational structure is distorted since  $D<0$ , which is unphysical, and  $\chi^2 \gg 1$ . If the perturbation is correctly accounted for, the deperturbed value of the rotational  $B$  parameter will somewhat change and might resemble the values of one of the  $N_2^+$  states. Finally,  $B=2.129 \text{ cm}^{-1}$  of system  $\beta_2^t$  exceeds any value in  $N_2$  and  $N_2^+$ , indicating that also this state is perturbed.

The values for the centrifugal distortion parameter  $D$ , as obtained from the fits, are unphysically large in many cases, which is indicative for weak or strong perturbations. The latter is certainly the case in system  $\alpha_3$  with  $D<0$ .

Another approach to assign the observed states, is to extrapolate the vibrational progression of known singlet *gerade* states. The only two states suitable for such an extrapolation are the  $y^1\Pi_g$ , and the  $k^1\Pi_g$  states. Both the  $a^1\Pi_g$  and  $a''^1\Sigma_g^+$  states have vibrational levels in the energy re-

gion investigated in this experiment, but these are far above the known levels, and extrapolation becomes insecure. The  $x^1\Sigma_g^-$  and  $z^1\Delta_g$  states are in principle not accessible from the intermediate  $c'_4{}^1\Sigma_u^+$ . This leaves only the  $y$  and  $k$  states for a vibronic extrapolation.

The deperturbed band origins of the  $y$  state are  $114\,073.34\text{ cm}^{-1}$  ( $v=0$ ),<sup>39</sup>  $115\,905.33\text{ cm}^{-1}$  ( $v=1$ ),<sup>40</sup> and  $117\,661.39\text{ cm}^{-1}$  ( $v=2$ ) (this paper). From this it is estimated, via a fit to a second order polynomial function, that the band origin of  $v=3$  is at  $\approx 119\,341\text{ cm}^{-1}$ . At  $119\,372\text{ cm}^{-1}$  a  $^1\Pi_g$  state is observed (see Table X). Moreover, the value of  $B=1.669\text{ cm}^{-1}$  of this level coincides with  $B=1.678\text{ cm}^{-1}$ , the value of  $A^2\Pi_g$  ( $v=3$ ) state of the  $N_2^+$  ion. This strongly suggests this band probes the  $y^1\Pi_g$  ( $v=3$ ) state.

The  $k$  state belongs to a Rydberg series converging to the ground state of the  $N_2^+$  ion. The vibrational spacings of the ionic state can be used to estimate the vibrational level energies of the  $k$  state. To validate this procedure, the spacing between  $v=0$  and  $v=1$  of these two states are compared. The two known deperturbed band origins of the  $k$  state are  $113\,723.58\text{ cm}^{-1}$  ( $v=0$ )<sup>39</sup> and  $115\,905.71\text{ cm}^{-1}$  ( $v=1$ ),<sup>40</sup> and therefore the spacing equals  $2181.13\text{ cm}^{-1}$ , which is only slightly more than the spacing in the ground state of  $N_2^+$ , being  $2174.75\text{ cm}^{-1}$ .<sup>49</sup> The spacings in the ground state of  $N_2^+$  of subsequent vibrational levels are, respectively,  $2142.23\text{ cm}^{-1}$  and  $2109.22\text{ cm}^{-1}$ .<sup>49</sup> This leads to estimated band origins of  $118\,048\text{ cm}^{-1}$  for  $v=2$  and  $120\,157\text{ cm}^{-1}$  for  $v=3$  of the  $k$  state. At  $118\,056\text{ cm}^{-1}$  and  $120\,164\text{ cm}^{-1}$  two bands are observed (see Table X). The rotational  $B$  parameters are comparable with the corresponding values of the ground state of  $N_2^+$ . These bands are therefore assigned to probe the  $v=2$  and  $v=3$  vibrational levels of the  $k^1\Pi_g$  state.

Some interactions have been taken explicitly into account. As is clear from the avoided crossings in Fig. 5 several states undergo a mutual interaction. The energies are fitted to the eigenvalues of the matrix, for every  $J$ ,

$$\begin{pmatrix} E_{\text{up}} & H \\ H & E_{\text{low}} \end{pmatrix} \Psi = E \Psi, \quad (3)$$

in which  $E_{\text{up}}$  and  $E_{\text{low}}$  are the unperturbed level energies of the upper and lower energy levels, respectively.  $H$  is the interaction parameter and is a constant when the two interacting states have the same symmetry properties (homogeneous interaction) and is dependent on  $J$  when they differ (heterogeneous interaction):

$$H \propto \sqrt{J(J+1)}, \quad (4)$$

in the case of an interaction between a  $^1\Sigma$  and a  $^1\Pi$  state, and

$$H \propto \sqrt{J(J+1)-2}, \quad (5)$$

when the interaction is between a  $^1\Pi$  and a  $^1\Delta$  state.

In the case of the interacting systems  $\beta_2^t$  and  $\beta_3^t$  it is not clear whether a homogeneous or heterogeneous interaction should be taken into account. Of both systems  $P$ ,  $Q$ , and  $R$  transitions are observed, as can be seen in Fig. 4, indicating that the states cannot be  $\Sigma$  states. The only other possibility

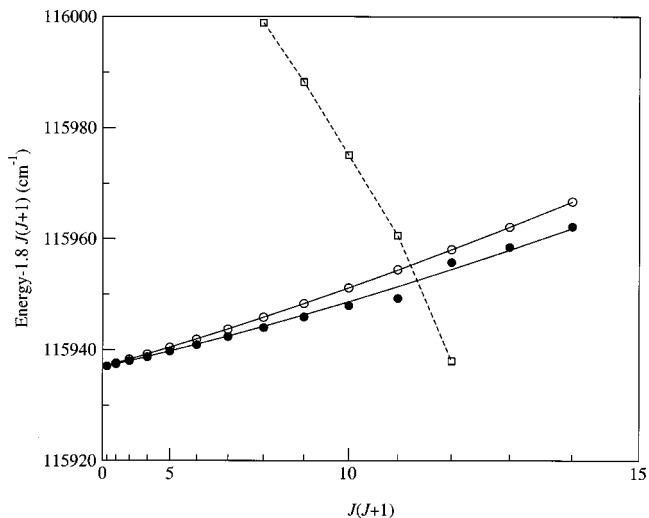


FIG. 6. The avoided crossing between systems  $\beta_2^t$  (filled markers) and  $\beta_3^t$  (open markers) is clearly seen. For clarity  $1.8 \times J(J+1)$  is subtracted from the level energies.

seems to be two interacting  $\Pi$  states. However, if one of the two is a  $\Pi$  state, the other state may be a  $\Delta$  state that gains transition strength from the interaction. The line strengths of both systems are equally strong around the interaction ( $J=8$ ), but is smaller for system  $\beta_2^t$  for the other values of  $J$ . This indeed indicates that the interaction strength to system  $\beta_2^t$  is gained by the mixing with system  $\beta_3^t$ . Therefore system  $\beta_3^t$  is identified as a  $\Pi$  state, but system  $\beta_2^t$  may be either a  $\Pi$  state or  $\Delta$  state. In Table XI the molecular constants are listed for both possibilities: a homogeneous interaction and a heterogeneous interaction. For both cases  $\chi^2=0.36$ , hampering a positive assignment for system  $\beta_2^t$ . It should be noted, that not only the assignment of  $\beta_2^t$  as a  $\Delta$  state explains the intensity behavior of the band, but also a  $\Pi$  with a low Franck-Condon factor in the transition from the intermediate state  $c'_4$ , would result in a similar intensity pattern. It is peculiar, that in neither band a transition to  $J=1$  could be observed (see Fig. 6), which is the lowest  $J$  supported by a  $\Pi$  state.

In Fig. 4 it is shown that the  $P$  transitions in the bands  $\beta_2^t-c'_4$  and  $\beta_3^t-c'_4$  are systematically weaker than the  $Q$  transitions, and these transitions are in turn less intense than the  $R$  transitions. As this effect is not observed in the other band systems, it cannot be ascribed to polarization effects of the several laser beams. Furthermore, in that case it would be expected that the effect is more strongly present for lower values of  $J$ , than high values. This seems, however, not to be the case; even for  $J=12$  this tendency is observed. In principle such intensity pattern could be a result of interfering matrix elements in the excitation of coupled states. The perturbing system  $\beta_2^t-\beta_3^t$  cannot be interpreted as an isolated two-level perturbation problem. The unphysical value for the rotational constant of  $\beta_2^t$  suggests that an additional unobserved state perturbs the system.

In Ref. 40 a perturbation was observed in the level energies of the ( $e$ ) component of the  $y^1\Pi_g$  ( $v=1$ ) and  $k^1\Pi_g$  ( $v=1$ ) states. It was stated that the perturber has to be a  $\Sigma^+$  state since the rotational progression of the ( $f$ ) component is

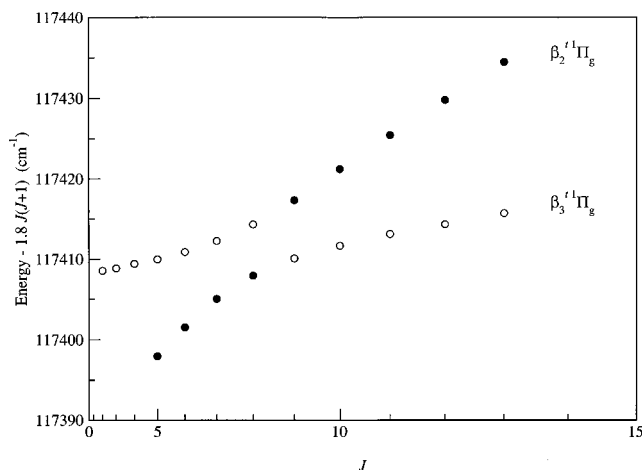


FIG. 7. The circles correspond to the  $k\ ^1\Pi_g$  ( $v=1$ ) state and the squares to the perturber; the  $\alpha_2\ ^1\Sigma_g^+$  state. Of the  $k$  state, both the ( $e$ ) (black circles) and the ( $f$ ) component (open circles) are depicted. The rotational progression of the  $f$  component is without irregularities, indicating that the perturbing state must be of  $^1\Sigma_g^+$  symmetry. From the levels around the crossing, it is estimated that the interaction parameter of this heterogeneous interaction  $H=0.3\text{ cm}^{-1}$ . The overall deviation from a straight line is due to the interaction with the  $y\ ^1\Pi_g$   $v=1$  state. Furthermore, the increasing energy difference between the ( $e$ ) and ( $f$ ) component, originates from  $\Lambda$  doubling.

not distorted. From Fig. 7 it is clear that  $\alpha_2$  causes an anti-crossing between  $J=11$  and  $12$ . The level energies of this state are determined up to  $J=12$  and therefore only the interaction parameter with the  $k$  state can be estimated. By applying Eq. (3) to the highest observed rotational levels, this parameter of the heterogeneous interaction is found to be  $H=0.3\text{ cm}^{-1}$ .

From Fig. 8 it is clear that another system of interacting states has been observed; states  $\alpha_4$ ,  $\alpha_5$ , and  $\alpha_6$  undergo a mutual interaction. At first glance it seems that the avoided crossing between  $\alpha_5$  and  $\alpha_6$  is the only perturbation to be accounted for, yet the level energies of the low rotational levels of  $\alpha_5$  are higher than expected. Furthermore, in band  $\alpha_4$   $D=1.1\times 10^{-3}\text{ cm}^{-1}$ ; three orders of magnitude higher

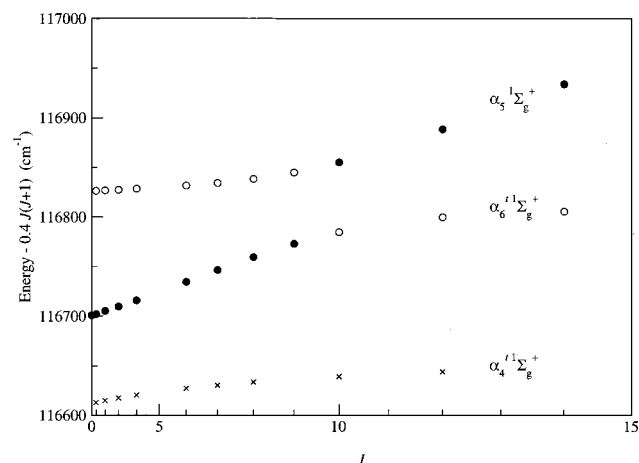


FIG. 8. The avoided crossing between systems  $\alpha_5$  (filled markers) and  $\alpha_6$  (open markers) is clearly seen, but also the repulsion of  $\alpha_4$  (crossed markers) and  $\alpha_5$  of low  $J$ . For clarity  $0.4\times J(J+1)$  is subtracted from the level energies.

TABLE XII. The molecular parameters of the interacting states  $\alpha_4$ ,  $\alpha_5$ , and  $\alpha_6$ . All values are in  $\text{cm}^{-1}$ . To identify the symmetry of  $\alpha_4$ , a heterogeneous interaction with  $\alpha_5$  and  $\alpha_6$  and a homogeneous interaction are taken into account.

System	$\nu$	$B$	$H_{\alpha_4\alpha_5}$	$H_{\alpha_4\alpha_6}$	$H_{\alpha_5\alpha_6}$
Heterogeneous interaction between $\alpha_4$ and $\alpha_5/\alpha_6$ assumed					
$\alpha_4$	116 614.39(7)	0.880(1)	1.77(2)	6.15(1)	
$\alpha_5$	116 707.20(7)	1.408(1)	1.77(2)		31.61(6)
$\alpha_6$	116 818.61(8)	1.701(1)		6.15(1)	31.61(6)
			$\chi^2=23.37$		
Homogeneous interaction between $\alpha_4$ and $\alpha_5/\alpha_6$ assumed					
$\alpha_4$	116 642.76(50)	0.469(3)	42.65(22)	0.38(26)	
$\alpha_5$	116 680.27(56)	1.579(4)	42.65(22)		36.27(9)
$\alpha_6$	116 817.56(15)	0.396(2)		0.38(26)	36.27(9)
			$\chi^2=6.70$		

than in  $N_2^+$ . It seems therefore, that also  $\alpha_4$  and  $\alpha_5$  repel each other. The avoided crossing between  $\alpha_5$  and  $\alpha_6$  can be investigated without taking  $\alpha_4$  into account, by leaving the low rotational levels of  $\alpha_5$  out of the analysis. Though it is certain that  $\alpha_5$  is a  $^1\Sigma_g^+$  state [ $P(1)$  has been observed],  $\alpha_6$  can still be either  $^1\Sigma_g^+$  or  $^1\Pi_g$  and hence, this interaction can still be homogeneous or heterogeneous. On the basis of the fitting procedures in which either of the interactions is incorporated, it is deduced that it is more probable that also the  $\alpha_6$  state is a  $^1\Sigma_g^+$  state. Finally, to deduce the symmetry of the  $\alpha_4$  state, all three bands have to be analyzed simultaneously. The energy levels of the three states are fitted to the eigenvalues of the  $3\times 3$  matrix,

$$\begin{pmatrix} E_{\alpha_4} & H_{\alpha_4\alpha_5} & H_{\alpha_4\alpha_6} \\ H_{\alpha_4\alpha_5} & E_{\alpha_5} & H_{\alpha_5\alpha_6} \\ H_{\alpha_4\alpha_6} & H_{\alpha_5\alpha_6} & E_{\alpha_6} \end{pmatrix} \Psi = E\Psi. \quad (6)$$

In the case that  $\alpha_4$  is a  $^1\Sigma_g^+$  state, all interactions are homogeneous and all interaction parameters are  $J$  independent. Alternatively, in the case that  $\alpha_4$  is a  $^1\Pi_g$  state, the interactions between  $\alpha_4$  and the two other states are homogeneous, and  $H_{\alpha_4\alpha_5}$  and  $H_{\alpha_4\alpha_6}$  depend on  $J$  as in Eq. (4). The results of both analyses are listed in Table XII. Note that the character of the interaction between  $\alpha_5$  and  $\alpha_6$  has been set to a homogeneous one on beforehand, but the value has been determined by fitting to Eq. (6). The assignment of  $^1\Sigma_g^+$  is more favorable than  $^1\Pi_g$  as  $\chi^2=6.70$  in the case of a homogeneous interaction and  $\chi^2=23.37$  if a heterogeneous interaction is assumed, but since in both cases  $\chi^2 \gg 1$ , the assignment is still tentative.

The emphasis in this study was laid on the spectroscopy, rather than intramolecular dynamics. Though linewidths of  $<0.10\text{ cm}^{-1}$  (laser linewidth) are feasible, as demonstrated in the detail study of Ref. 40, the lines are usually intensity broadened. As the accuracy of the calibration is  $\approx 0.20\text{ cm}^{-1}$ , no special attention was given to produce minimal linewidths. This might have concealed broadening effects which could have been ascribed to fast dynamical processes.

Besides line broadening, missing lines may also indicate the presence of predissociation. The spectra are retrieved by ionizing the excited molecules. In the case of decay processes, the ionization laser beam has to compete with the loss rates of these processes. This may lead to lower intensities even to the point of vanishing lines.<sup>50</sup> Though not all possible transitions have been observed, no special attention was given to these missing lines in the present study.

At energies around 116 000 cm<sup>-1</sup>, features have been observed which could not be assigned, not even in terms of rotational quantum numbers. It might be that these features arise from multiple photon absorptions, e.g., XUV+2 Vis. In a future experiment these features may be investigated in a systematic way.

#### IV. CONCLUSION

In this paper nineteen rovibrational progressions of *gerade* symmetry are reported. Fifteen progressions have been observed for the first time. The states have been investigated by means of an XUV+VIS laser-scheme. Even though a complete assignment is not possible yet, due to the lack of *ab initio* calculations of spectroscopic accuracy, a symmetry assignment has been made to 12 vibrational levels, based on the observed transitions. Seven of these assignments are tentative. Three vibrational states have been assigned as belonging to known electronic states;  $y^1\Pi_g$  ( $v=3$ ) and  $k^1\Pi_g$  ( $v=2,3$ ). In the current experiment, the intermediate state  $c'_4^1\Sigma_u^+$  is used which has Rydberg character. One might obtain new insights when a state with valence character is used, e.g.,  $b^1\Pi_g$  ( $v=1$ ). The  $b$  state is a  $\Pi$  state which enables the probing of  $\Delta$  states in contrast to the  $c'_4^1\Sigma_u^+$  state. Furthermore, the valence character will provide different Franck-Condon overlaps with the *gerade* states, enabling to probe other states than in the case of  $c'_4$ .

#### ACKNOWLEDGMENTS

Financial support from the Earth Observation (EO) program of the Space Research Organization Netherlands (SRON) and the Molecular Atmospheric Physics (MAP) program of the Netherlands Foundation for Research of Matter (FOM) is gratefully acknowledged.

<sup>1</sup>R. E. Worley, Phys. Rev. **64**, 207 (1943).

<sup>2</sup>P. G. Wilkinson and N. B. Houk, J. Chem. Phys. **24**, 528 (1956).

<sup>3</sup>S. G. Tilford and P. G. Wilkinson, J. Mol. Spectrosc. **12**, 231 (1964).

<sup>4</sup>H. Lefebvre-Brion, Can. J. Phys. **47**, 541 (1969).

<sup>5</sup>K. Dressler, Can. J. Phys. **47**, 547 (1969).

<sup>6</sup>P. K. Carroll and C. P. Collins, Can. J. Phys. **47**, 563 (1969).

<sup>7</sup>P. K. Carroll and K. Yoshino, J. Phys. B **5**, 1614 (1972).

<sup>8</sup>D. Stahel, M. Leoni, and K. Dressler, J. Chem. Phys. **79**, 2541 (1983).

<sup>9</sup>T. Lyman, Astrophys. J. **33**, 98 (1911).

<sup>10</sup>R. T. Birge and J. J. Hopfield, Astrophys. J. **68**, 257 (1928).

<sup>11</sup>J. T. Vanderslice, S. G. Tilford, and P. G. Wilkinson, Astrophys. J. **141**, 395 (1965).

<sup>12</sup>R. E. Miller, J. Opt. Soc. Am. **60**, 171 (1970).

<sup>13</sup>T. Trickl, D. Proch, and K. L. Kompa, J. Mol. Spectrosc. **162**, 184 (1993).

<sup>14</sup>J.-Y. Roncin, J.-L. Subtil, and F. Launay, J. Mol. Spectrosc. **188**, 128 (1998).

<sup>15</sup>A. G. Gaydon, Proc. R. Soc. London, Ser. A **182**, 286 (1944).

<sup>16</sup>A. G. Gaydon and R. E. Worley, Nature (London) **153**, 747 (1944).

<sup>17</sup>A. G. Gaydon and R. Herman, Proc. R. Soc. London **58**, 292 (1946).

<sup>18</sup>R. Herman, Ann. Phys. (Paris) **20**, 241 (1945).

<sup>19</sup>R. Herman and A. G. Gaydon, J. Phys. Radium **7**, 121 (1946).

<sup>20</sup>R. A. McFarlane, Phys. Rev. **140**, A1070 (1965).

<sup>21</sup>R. A. McFarlane, IEEE J. Quantum Electron. **2**, 229 (1966).

<sup>22</sup>R. A. McFarlane, Phys. Rev. **146**, 37 (1966).

<sup>23</sup>R. A. McFarlane, *Stimulated-Emission Spectroscopy of Some Diatomic Molecules*, edited by P. L. Kelly, B. Lax, and P. E. Tannenwald (McGraw-Hill, New York, 1966), pp. 655–663.

<sup>24</sup>R. S. Mulliken, *The Threshold of Space*, edited by M. Zelikoff (Pergamon, New York, 1957), pp. 169–179.

<sup>25</sup>H. Lefebvre-Brion and C. M. Moser, J. Chem. Phys. **43**, 1394 (1965).

<sup>26</sup>K. Dressler and B. L. Lutz, Phys. Rev. Lett. **19**, 1219 (1967).

<sup>27</sup>J. W. Ledbetter, Jr., J. Mol. Spectrosc. **42**, 100 (1972).

<sup>28</sup>T. Suzuki and M. Kakimoto, J. Mol. Spectrosc. **93**, 423 (1982).

<sup>29</sup>Th. F. Hanisco and A. C. Kummel, J. Phys. Chem. **95**, 8565 (1991).

<sup>30</sup>Y. Kawamoto, M. Fujitake, and N. Ohashi, J. Mol. Spectrosc. **185**, 330 (1997).

<sup>31</sup>D. C. Duncan, Astrophys. J. **62**, 145 (1925).

<sup>32</sup>E. T. S. Appleyard, Phys. Rev. **41**, 254 (1932).

<sup>33</sup>A. van der Ziel, Physica (Utrecht) **1**, 513 (1934).

<sup>34</sup>A. Lofthus, J. Chem. Phys. **25**, 494 (1956).

<sup>35</sup>J. Kaplan, Phys. Rev. **46**, 534 (1934).

<sup>36</sup>J. Kaplan, Phys. Rev. **46**, 631 (1934).

<sup>37</sup>J. Kaplan, Phys. Rev. **47**, 259 (1935).

<sup>38</sup>A. Lofthus and R. S. Mulliken, J. Chem. Phys. **26**, 1010 (1957).

<sup>39</sup>P. K. Carroll and K. V. Subbaram, Can. J. Phys. **53**, 2198 (1975).

<sup>40</sup>A. de Lange and W. Ubachs, Chem. Phys. Lett. **310**, 471 (1999).

<sup>41</sup>A. Lofthus, Can. J. Phys. **35**, 216 (1957).

<sup>42</sup>H. H. Michels, in *Electronic Structure of Excited States of Selected Atmospheric Systems*, edited by J. Wm. McGowan, The Excited State in Chemical Physics, Vol. II, Chap. 3 (Wiley, New York, 1980).

<sup>43</sup>W. Ubachs, Chem. Phys. Lett. **268**, 210 (1997).

<sup>44</sup>P. F. Levelt and W. Ubachs, Chem. Phys. **163**, 263 (1992).

<sup>45</sup>A. Bernard, M. Larzillière, C. Effantin, and A. J. Ross, Astrophys. J. **413**, 829 (1993).

<sup>46</sup>D. W. Ferguson and K. Narahari Rao, J. Mol. Spectrosc. **153**, 599 (1992).

<sup>47</sup>M. B. Radunsky and R. J. Saykally, J. Chem. Phys. **87**, 898 (1987).

<sup>48</sup>W. Benesch, D. Rivers, and J. Moore, J. Opt. Soc. Am. **70**, 792 (1980).

<sup>49</sup>A. Lofthus and P. H. Krupenie, J. Phys. Chem. Ref. Data **6**, 113 (1977).

<sup>50</sup>K. S. E. Eikema, W. Hogervorst, and W. Ubachs, Chem. Phys. **181**, 217 (1994).